

# Synthesis, Structure and Properties of Related Microporous *N,N'*-Piperazinebismethylenephosphonates of Aluminum and Titanium

Christian Serre,<sup>\*,†</sup> John A. Groves,<sup>‡</sup> Philip Lightfoot,<sup>‡</sup> Alexandra M. Z. Slawin,<sup>‡</sup> Paul A. Wright,<sup>‡</sup> Norbert Stock,<sup>§</sup> Thomas Bein,<sup>||</sup> Mohamed Haouas,<sup>†</sup> Francis Taulelle,<sup>†</sup> and Gérard Férey<sup>†</sup>

*Institut Lavoisier, UMR CNRS 8180, Université de Versailles St-Quentin-en-Yvelines, 45 Avenue des Etats-Unis 78035 Versailles Cedex, France, School of Chemistry, University of St. Andrews, North Haugh, St. Andrews, Fife KY16 9ST, United Kingdom, Institut für Anorganische Chemie, University of Kiel, Otto-Hahn-Platz 6/7, 24118 Kiel, Germany, and Department of Chemistry, Ludwig-Maximilians-University, Butenandstr. 5-13, Haus E, 81377 Munich, Germany*

Received September 26, 2005. Revised Manuscript Received November 14, 2005

A porous framework titanium(IV) *N,N'*-piperazinebis(methylenephosphonate) (MIL-91(Ti)) and its aluminum analogue have been prepared under hydrothermal conditions (MIL = Material Institut Lavoisier). The structure of the aluminum analogue,  $\text{AlOH}(\text{H}_2\text{L})\cdot n\text{H}_2\text{O}$  ( $n \sim 3$ ,  $\text{L} = \text{O}_3\text{P}-\text{CH}_2-\text{NC}_4\text{H}_8\text{N}-\text{CH}_2-\text{PO}_3$ ) was solved from a small single crystal and refined against laboratory powder X-ray diffraction data. The structure of the titanium form ( $\text{TiO}(\text{H}_2\text{L})\cdot n\text{H}_2\text{O}$  ( $n \sim 4.5$ )) was determined using the structure of the aluminum form as a starting model and refining it against laboratory X-ray data. Their structures are built up from trans corner-sharing chains of  $\text{TiO}_6$  or  $\text{AlO}_6$  octahedra linked together in two directions via the diphosphonate groups. In each case this gives rise to a three-dimensional hybrid network with small channels along the *b* axis, filled with free water molecules. Thermogravimetric analysis and X-ray thermodiffractionometry of the samples reveal that water is lost reversibly below 423 K and that both structures are stable up to 463 K. Dehydration gives porous solids (pore size  $\sim 3.5 \times 4.0 \text{ \AA}^2$ ) which adsorb nitrogen at 77 K to give Langmuir surface areas close to  $500 \text{ m}^2\cdot\text{g}^{-1}$ . Crystal data for MIL-91(Ti) are as follows: space group *C2/m* (No. 12) with  $a = 19.415(2) \text{ \AA}$ ,  $b = 7.071(1) \text{ \AA}$ ,  $c = 11.483(1) \text{ \AA}$ ,  $\beta = 92.78(1)^\circ$ ,  $V = 1574.70(1) \text{ \AA}^3$ , and  $Z = 2$ . Crystal Data for MIL-91(Al) are as follows: space group *C2/m* (No. 12) with  $a = 18.947(2) \text{ \AA}$ ,  $b = 6.915(1) \text{ \AA}$ ,  $c = 11.295(1) \text{ \AA}$ ,  $\beta = 90.45(1)^\circ$ , and  $V = 1479.90(1) \text{ \AA}^3$ .

## 1. Introduction

The synthesis of hybrid inorganic–organic porous solids is of great current interest.<sup>1–3</sup> Associating metal cations and oxy or hydroxy metal coordination polyhedra with different organic linkers permits the creation of a wide variety of porous solids with distinctive pore geometries and physical properties that depend on the metal species included. While the majority of synthetic efforts are being devoted to the synthesis of porous metal carboxylates such as the metal–organic framework porous solids reported by Yaghi and co-workers<sup>1</sup> or the MIL-*n* solids of Férey et al.<sup>4</sup> a steadily growing number of porous or layered metallodiphosphonates have been reported with a range of di- and trivalent metals, including first row transition metals, group 13 metals, and rare earth metals.<sup>5–16</sup> By contrast, relatively few tetravalent

metal-based hybrid inorganic–organic framework solids have been reported. Most of these have arisen from the work of Clearfield and co-workers who have prepared a series of zirconium phosphonates,<sup>17,18</sup> some of which exhibit porosity.<sup>12,19</sup> We have also embarked upon a systematic study of the titanium and zirconium diphosphonate systems under hydrothermal conditions and recently reported several solids

\* To whom correspondence should be addressed. E-mail: serre@chimie.uvsq.fr, ferey@chimie.uvsq.fr.

<sup>†</sup> Université de Versailles St-Quentin-en-Yvelines.

<sup>‡</sup> University of St. Andrews.

<sup>§</sup> University of Kiel.

<sup>||</sup> Ludwig-Maximilians-University.

- (1) Eddaoudi, M.; Moler, D. B.; Li, H.; Chen, B.; Reineke, T.; O'Keefe, M.; Yaghi, O. M. *Acc. Chem. Res.* **2001**, *34*, 319.
- (2) Férey, G. *Chem. Mater.* **2001**, *13*, 3084.
- (3) Feng, S.; Xu, R. *Acc. Chem. Res.* **2001**, *34*, 239.
- (4) Férey, G.; Mellot-Draznieks, C.; Serre, C.; Millange, F. *Acc. Chem. Res.* **2005**, *38*, 217–225.

- (5) Cavellec, M.; Serre, C.; Robino, J.; Noguès, M.; Grenèche, J. M.; Férey, G. *J. Solid State Chem.* **1999**, *147*, 122.
- (6) Distler, A.; Lohse, D. L.; Sevov, S. C. *J. Chem. Soc., Dalton Trans.* **1999**, 1805.
- (7) Dumas, E.; Sassoie, C.; Smith, K. D.; Sevov, S. C. **2002**, *41*, 4029.
- (8) Serpaggi, F.; Férey, G. *J. Mater. Chem.* **1998**, *8*, 2749.
- (9) Riou, D.; Roubeau, O.; Férey, G. *Microporous Mesoporous Mater.* **1998**, *23*, 23.
- (10) Soghomonian, V.; Chen, Q.; Haushalter, R. C.; Zubieta, J. *Angew. Chem., Int. Ed. Engl.* **1995**, *34*, 223.
- (11) Serre, C.; Férey, G. *J. Mater. Chem.* **2002**, *12*, 2367.
- (12) Byrd, H.; Clearfield, A.; Poojary, D.; Reis, K. P.; Thompson, M. E. *Chem. Mater.* **1996**, *8*, 2239.
- (13) Adair, B.; Delgado, G. D.; Delgado, J. M.; Cheetham, A. K. *Solid State Sci.* **2000**, *2*, 119.
- (14) Devi, R. N.; Wormald, P.; Cox, P. A.; Wright, P. A. *Chem. Mater.* **2004**, *16*, 2229.
- (15) Groves, J. A.; Wright, P. A.; Lightfoot, P. *Inorg. Chem.* **2005**, *44*, 1736.
- (16) Harvey, H. G.; Slater, B.; Attfield, M. P. *Chem.—Eur. J.* **2004**, *10*, 3270.
- (17) Clearfield, A., Karlin, K. D., Eds.; John Wiley and Sons: New York, 1998; Vol. 47, pp 371–510.
- (18) Clearfield, A. *Curr. Opin. Solid State Mater. Sci.* **1996**, *1*, 268.

with one- or three-dimensional structures but without porosity.<sup>11,20–22</sup> This paper deals with the synthesis, structure determination, solid-state NMR characterization, thermal behavior, and sorption properties of a titanium diphosphonate with significant porosity: MIL-91(Ti) or  $\text{TiO}(\text{H}_2\text{L})\cdot n\text{H}_2\text{O}$  ( $n \sim 4.5$ ) and the synthesis and characterization of its aluminum analogue,  $\text{AlOH}(\text{H}_2\text{L})\cdot n\text{H}_2\text{O}$  ( $n \sim 3$ ), prepared in parallel synthetic studies of aluminum phosphonates. In the latter material, the  $[\text{TiO}]^{2+}$  group is replaced by  $[\text{AlOH}]^{2+}$ . A structural model obtained from small single crystals of the aluminum form has been used for structural solution of the titanium form by refinement of the model against X-ray powder diffraction (XRD) data.

## 2. Experimental Section

**Synthesis and Chemical Analysis.** MIL-91(Ti). MIL-91(Ti) was hydrothermally synthesized ( $T = 493$  K, autogenous pressure for 4 days) from a mixture of  $\text{TiO}_2\cdot\text{H}_2\text{O}$  (see procedure below),  $N,N'$ -piperazinebismethylenephosphonic acid,<sup>23</sup> HF (Prolabo Normapur 40%), and  $\text{H}_2\text{O}$  in the molar ratio 1:1:1:280 introduced in this order without stirring in a Teflon-lined steel autoclave. The hydrous titanium dioxide  $\text{TiO}_2\cdot\text{H}_2\text{O}$  was prepared from the reaction of a strongly acidic solution of  $\text{TiCl}_4$  (Aldrich, 99%) in HCl (Prolabo, 36%) with ammonia (Prolabo, 20%) at room temperature: the precipitate was washed several times with demineralized water and dried at 373 K.

After hydrothermal treatment of the gel at 493 K, white, microcrystalline MIL-91(Ti) is obtained with a yield of 75% based on titanium. The pH remains acidic ( $<2$ ) during the reaction. Quantitative analyses indicated titanium, phosphorus, carbon, and nitrogen values (11.92, 14.52, 16.70, and 6.67 wt %, respectively) in agreement with the theoretical values (11.46, 14.79, 17.18, and 6.68 wt %).

MIL-91(Al). The  $N,N'$ -piperazinebismethylphosphonic acid  $\text{H}_2\text{O}_3\text{P}-\text{CH}_2-\text{NC}_4\text{H}_8\text{N}-\text{CH}_2-\text{PO}_3\text{H}_2$  was synthesized starting from piperazine hexahydrate using a Mannich type reaction. In a typical reaction 0.1 mol (19.4 g) piperazine hexahydrate and 0.2 mol of phosphorous phosphoric acid (16.4 g) are dissolved in a mixture of 10 mL of  $\text{H}_2\text{O}$  and 10 mL of concentrated HCl. The solution is heated to reflux, and 0.222 mol of an aqueous solution of formaldehyde (37%, 22 mL) is slowly added. After 2 h the reaction is stopped, and the mixture is slowly cooled to room temperature. The product is obtained as a microcrystalline powder.

The aluminum analogue of MIL-91 was first prepared as a microcrystalline powder by the reaction of aluminum chloride hydrate ( $\text{AlCl}_3\cdot 6\text{H}_2\text{O}$ , Aldrich) with  $N,N'$ -piperazinebismethylenephosphonic acid. In a typical preparation, the phosphonic acid and aluminum chloride were mixed for 1 h at 343 K in water in the molar ratio 1:1.33:900. The pH was raised to 5 with the dropwise addition of a 1.0 M sodium hydroxide solution. The resulting mixture was treated hydrothermally in a poly(tetrafluoroethylene) lined autoclave at 463 K for 130 h, giving a white crystalline powder MIL-91(Al). Selected area energy-dispersive X-ray analysis of crystals of the product indicated an Al:P ratio of 1:2. The measured carbon, hydrogen, and nitrogen values (17.1, 5.7, and 6.7 wt %, respectively) were slightly lower than the theoretical values (19.2, 5.9, and 7.4 wt %).

In a subsequent preparation, the phosphonic acid was reacted with aluminum phosphate ( $\text{AlPO}_4\cdot 3\text{H}_2\text{O}$ , BDH) in water (molar ratio 1:1:700) at 463 K for 120 h. This also resulted in the preparation of MIL-91(Al), as determined by XRD, containing a minor impurity. In this preparation, however, the MIL-91(Al) crystallized in the form of very small single crystals that were subsequently successfully examined by single-crystal diffractometry.

**X-ray Powder Diffraction.** The XRD patterns were collected on a D5000 ( $\theta-2\theta$  mode) Siemens diffractometer with  $\lambda\text{Cu}(\text{K}\alpha_1, \text{K}\alpha_2) = 1.5406, 1.5444$  Å. To minimize the preferred orientation effect on the XRD pattern, the fine powders were mounted in a top-loaded MacMurdie type sample holder, which reduced the effects of preferred orientation.

**Thermal Analysis.** Thermogravimetric analysis (TGA) was performed on a TA-Instrument type 2050 analyzer apparatus, under an oxygen atmosphere. Nitrogen adsorption isotherms were measured for MIL-91(Ti) on a volumetric Micromeritics ASAP 2010 instrument, and for MIL-91(Al) they were measured on a gravimetric IGA porosimeter. The solids were dehydrated under vacuum at 413 K (Al) or 473 K (Ti) before measuring the isotherm to remove physisorbed water without destroying the structure.

**Solid-State NMR.**  $^{31}\text{P}$  and  $^{27}\text{Al}$  magic-angle spinning (MAS) NMR studies of as-prepared MIL-91(Al) were performed on a Varian Infinityplus 500 MHz spectrometer, fitted with a standard 4 mm probe, at resonance frequencies of 130.324 and 202.466 MHz for  $^{27}\text{Al}$  and  $^{31}\text{P}$ , respectively. A 1 M aqueous solution of  $\text{Al}(\text{NO}_3)_3\cdot 9\text{H}_2\text{O}$  (0 ppm) and calcium hydrogenphosphate dihydrate (Brushite) ( $-1.2$  ppm) were used as chemical shift standards. Samples were spun at the magic angle at speeds of 10–12 kHz. Pulse durations were 1.0 and 4.0  $\mu\text{s}$ , and pulse delays were 0.4 and 1.0 s for  $^{27}\text{Al}$  and  $^{31}\text{P}$ , respectively.

NMR spectra of MIL-91(Ti) were acquired on a Bruker Avance 500 spectrometer with an 11.7 T field, equipped with Bruker MAS 4 mm and 2.5 mm probes, with resonance frequencies for  $^1\text{H}$ ,  $^{13}\text{C}$ , and  $^{31}\text{P}$  of 500.13, 125.77, and 202.46 MHz, respectively. The single pulse  $^1\text{H}$  MAS experiment was carried out using a  $\pi/2$  pulse width of 3.25  $\mu\text{s}$ , a repetition times of 4 s, and spectral widths of 100 kHz. The MAS speed employed was 30 kHz using a 2.5 mm  $\text{ZrO}_2$  rotor. The  $^{13}\text{C}\{^1\text{H}\}$  cross-polarization magic-angle spinning (CP-MAS) spectrum was achieved using a 4 mm  $\text{ZrO}_2$  rotor at a sample rotation frequency of 5 kHz. The following conditions were used: contact time of 5 ms, relaxation delay of 4 s,  $^1\text{H}$  radio frequency field of 44 kHz, and high power proton decoupling of 25 kHz. Single pulse  $^{31}\text{P}$  MAS and  $^{31}\text{P}-^{31}\text{P}$  double quantum (DQ) experiments were run with spinning at frequencies of 30 and 12.5 kHz, respectively. Quantitative conditions were applied for the single pulse experiment using a  $\pi/4$  pulse and 60 s as the relaxation delay. The optimum repetition time for  $\pi/2$  was found to be 85 s. The  $^{31}\text{P}-^{31}\text{P}$  DQ MAS correlation spectrum was obtained using the POSTC7 sequence.<sup>24</sup> The two-dimensional spectrum was collected with 48  $t_1$  increments and 80 transients each using the hypercomplex method.<sup>25</sup> Presaturation pulses prior to the first pulse of the DQ sequence were used to reduce the recycle delay to 20 s without saturation. The excitation and conversion periods were optimized and correspond to 1.44 ms. All spectra were referenced to the chemical shifts of adamantane at 1.7 ppm for  $^1\text{H}$  and 38.3 ppm for  $^{13}\text{C}$  and of  $\text{NH}_4\text{H}_2\text{PO}_4$  at 0.0 ppm for  $^{31}\text{P}$  relative to the standards tetramethylsilane and 85 wt %  $\text{H}_3\text{PO}_4$  in water, respectively. Decomposition of spectra was achieved using the dm2004 NMR simulation software.<sup>26</sup>

(19) Wang, S.; Clearfield, A.; Heising, J. M. *J. Am. Chem. Soc.* **2003**, *125*, 10375.

(20) Serre, C.; Riou, D.; Férey, G. *C. R. Acad. Sci., Ser. IIC* **1999**, *2*, 85.

(21) Serre, C.; Férey, G. *Inorg. Chem.* **1999**, *38*, 5370.

(22) Serre, C.; Férey, G. *Inorg. Chem.* **2001**, *40*, 5350.

(23) Moedritzer, K.; Irani, R. R. *J. Org. Chem.* **1966**, *31*, 1603.

(24) Hohwy, M.; Jakobsen, H. J.; Eden, M.; Levitt, M. H.; Nielsen, N. C. *J. Chem. Phys.* **1998**, *108*, 2686.

(25) States, D. J.; Haberhorn, R. A.; Ruben, D. J. *J. Magn. Reson.* **1982**, *48*, 286.

**Structure Determination.** The structure of MIL-91(Al) prepared using aluminum phosphate as the aluminum source was solved from laboratory single-crystal data on a very small crystal ( $100 \times 30 \times 10 \mu\text{m}$ ) using direct methods in the SHELXS program and refined using the SHELXL-97 code. High  $R$  factors at this stage ( $R_1$ (all data) = 0.165,  $wR_2$  = 0.323) are thought to be due to the very small crystal size and the presence of some disorder in the structure. Two crystallographically distinct sites were found for the phosphonate ligands, one of which (that including P(1)) shows disorder over two equivalent orientations. Hydrogen atoms were located bound to the nitrogen atoms of both crystallographically distinct bisphosphonate ligands and on the bridging oxygen atoms in the Al–OH–Al–OH chains. Water molecules were located within the pores by difference Fourier methods.

To confirm that the single-crystal structure is correct and corresponds to the structure of the bulk MIL-91(Al) phase, the powder pattern of the phase pure material prepared using aluminum chloride as the aluminum source was matched using the single-crystal structure as a starting model for the framework. The profile was indexed with the DICVOLGV program,<sup>27</sup> giving a monoclinic solution consistent with the space group  $C2/m$  (No. 12) observed by single-crystal diffraction. The model was successfully refined against the data using the FULLPROF program<sup>28</sup> in the WINPLOTR package,<sup>29</sup> and difference Fourier analysis was performed to locate the water molecules.<sup>30</sup> The profile fitting was performed with a six parameter polynomial function to adjust the background and a pseudo-Voigt function to determine the peak profile. Two asymmetry parameters, an overall thermal parameter and a preferred orientation correction parameter, were used during refinements. Soft distance and angle constraints were also applied. The preferred orientation vector was chosen as the direction parallel to the pores ( $c$  axis). The final reliability factors are satisfactory ( $R_{\text{Bragg}}$  = 8.5% and  $R_p$  = 11.6%).

A similar approach was adopted for the structure analysis of MIL-91(Ti), again using the single-crystal structure of MIL-91(Al) as a starting point, but in this case replacing AlOH structural units by titanyl groups. A small amount of crystalline titanium dioxide was observed in the X-ray pattern and matched by including anatase as a second phase during the refinement. The reliability factors are  $R_{\text{Bragg}}$  = 10.7% and  $R_p$  = 13.1%. Details of the structure refinements from laboratory powder data are summarized in Table 1. The final Rietveld plots are reported in Figure 1. Atomic coordinates are reported in Table 2 while bond distances are reported in Table 3.

### 3. Results and Discussion

MIL-91(Ti, Al) is a framework solid, the structure of which is illustrated in Figure 2a–c for the aluminum analogue. The framework structure is built up from the linkage of chains of corner-sharing  $\text{TiO}_6$  or  $\text{Al}(\text{OH})_2\text{O}_4$  octahedra and protonated bisphosphonate groups ( $\text{PO}_3\text{---CH}_2\text{---NHC}_4\text{H}_{10}\text{NH---CH}_2\text{---PO}_3$ ), with two types of linkages: M–X–M and

**Table 1. Crystal Data and Structure Refinement Parameters for MIL-91**

formula	$\text{TiO}(\text{O}_3\text{P---CH}_2\text{---NHC}_4\text{H}_{10}\text{NH---CH}_2\text{---PO}_3) \cdot n\text{H}_2\text{O}$ ( $n \sim 3.6$ )	$\text{Al}(\text{OH})(\text{HO}_3\text{P---CH}_2\text{---NC}_4\text{H}_{10}\text{N---CH}_2\text{---PO}_3\text{H}) \cdot n\text{H}_2\text{O}$ ( $n \sim 3$ )
chemical formula	419	399
weight ( $\text{g}\cdot\text{mol}^{-1}$ )		
calculated density ( $\text{g}\cdot\text{cm}^{-3}$ )	1.77	1.79
crystal system	monoclinic	monoclinic
space group	$C2/m$	$C2/m$
$a$ (Å)	19.415(2)	18.947(2)
$b$ (Å)	7.071(1)	6.915(1)
$c$ (Å)	11.483(1)	11.295(1)
$\beta$ (deg)	92.78(1)	90.45(1)
$V$ (Å <sup>3</sup> )	1574.71(1)	1479.90(1)
$Z$	4	4
figures of Merit	$M_{20} = 13; F_{20} = 22$	$M_{20} = 16; F_{20} = 32$
radiation ( $\lambda\text{Cu}$ (Å): $K\alpha_1, K\alpha_2$ )	1.540 59, 1.544 39	1.540 59, 1.544 39
$2\theta$ range (deg)	6.5–70	7.15–60
reflections	388	289
atoms	19	18
intensity-dependent parameters	42	40
profile parameters	20	20
$R_p$	0.131	0.116
$R_{\text{WP}}$	0.180	0.155
$R_{\text{exp}}$	0.075	0.086
$R_B$	0.108	0.085
$R_F$	0.073	0.078
secondary phase	$\text{TiO}_2$ anatase	
excluded areas	37.6–38.8 and 43.9–45.10 (most intense reflections of the Al sample holder)	37.6–38.8 and 43.9–45.10 (most intense reflections of the Al sample holder)

M–O–P (M = Ti, Al; X = O, OH). Each  $\text{PO}_3\text{C}$  group of the diphosphonate units acts as a bridging linker and shares two of its three oxygen atoms with the metal cations; the third oxygen atom occupies a terminal position (Figure 3). Bond lengths from the single-crystal data of MIL-91(Al) suggest this corresponds to a P=O group in this structure. An approximate  $\text{MX}(\text{O}_3\text{P---CH}_2\text{---NHC}_4\text{H}_{10}\text{NH---CH}_2\text{---PO}_3) \cdot n\text{H}_2\text{O}$  ( $n \sim 4.5$  or 3; MX = TiO, AlOH) formula is thus proposed for the two solids. The piperazine organic spacers adopt a chair configuration and relate neighboring chains along the  $a$  and  $c$  axes. Such chains, which are similar to those found in the mineral tancoite,<sup>31</sup> are well-known in titanium and aluminum phosphate chemistry.

**MIL-91(Al).** The single-crystal structure solution of MIL-91(Al) indicates that the protonated nitrogens of the piperazine are hydrogen-bonded to terminal oxygens on the phosphonate groups (N1–O4, 2.67 Å; N2–O5, 2.68 Å) so that H bonds as well as covalent bonds hold the framework together. The arrangement of the piperazine-based ligands links neighboring Al–OH–Al chains leaving channels along the  $b$  axis with free dimensions of around  $3.5 \times 3.5$  Å. The packing of ligands is such that there is no significant porosity along either the  $a$  or the  $c$  axes. Interatomic distances from the single-crystal data (and the powder X-ray refinement) are within the expected ranges (Al–O, 1.87–1.93 Å; P–O, 1.49–1.52 Å; P–C, 1.82–1.84 Å). Solid-state NMR (Supporting Information) is consistent with the crystal structure of MIL-91(Al). The <sup>27</sup>Al MAS NMR spectrum has a typical quadrupolar line shape similar to that seen previously in aluminum phosphonates that have a related Al–OH–Al chain. The <sup>31</sup>P MAS NMR of the sample of MIL-91(Al) that

(26) Massiot, D.; Fayon, F.; Capron, M.; King, I.; LeCalve, S.; Alonso, B.; Durand, J. O.; Bujoli, B.; Gan, Z.; Hoatson, G. *Magn. Reson. Chem.* **2002**, *40*, 70.

(27) Boulouf, A.; Lötter, D. *J. Appl. Crystallogr.* **1991**, *24*, 987.

(28) Rodriguez-Carvajal, J. "FULLPROF: A Program for Rietveld Refinement and Pattern Matching Analysis." *Abstracts of the Satellite Meeting on Powder Diffraction of the XV Congress of the IUCr*, Toulouse, France, 1990; p 127.

(29) Roisnel, T.; Rodriguez-Carvajal, J. *Materials Science Forum, Proceedings of the European Powder Diffraction Conference (EPDIC 7)* **2001**, *378–381*, 118–123.

(30) Sheldrick, G. M. *SHELXS97 and SHELXL97*; Software package for the Crystal Structure Determination; University of Göttingen: Göttingen, Germany, 1997.

(31) Hawthorne, F. C. *Acta Crystallogr., Sect. B* **1994**, *50*, 481.

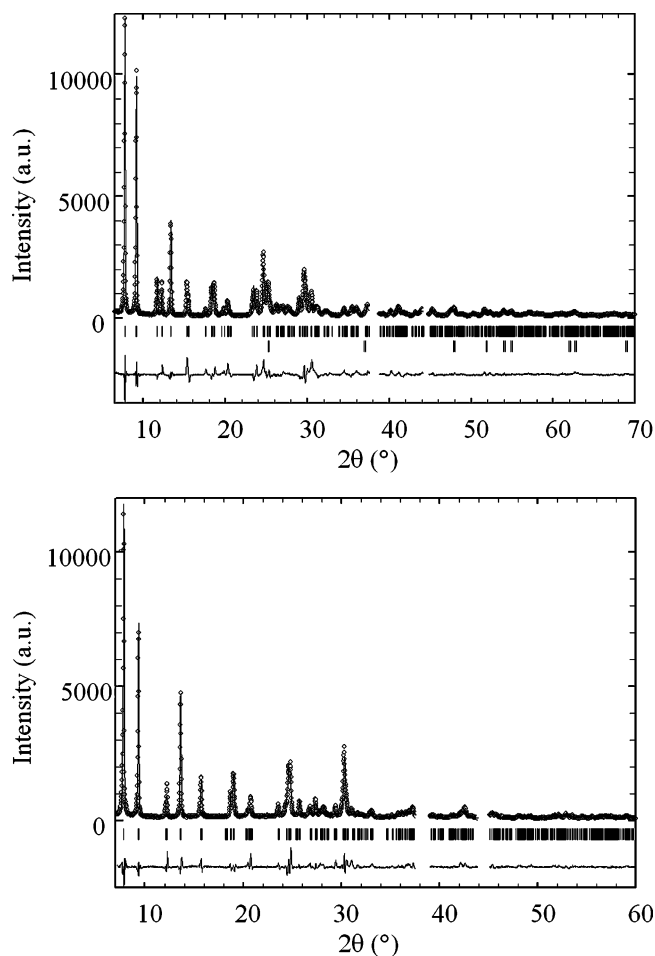


**Figure 1.** Rietveld plots of (a) MIL-91(Ti) and (b) MIL-91(Al).

contains larger crystals, which has some phosphate impurity, shows (in addition to spinning sidebands) two sharp peaks,  $\delta = 2.0$  and  $6.3$  ppm (from the phosphonate) and a smaller peak at  $-19.4$  ppm (from the phosphate). From the powder sample, there is just one broader peak,  $\delta = 1.1$  ppm.

The thermal behavior of MIL-91(Al) shows (Figure 4) a weight loss of 14.5 wt % below 473 K, corresponding to loss of physisorbed water molecules from the channels (ca. three water molecules per formula unit). If the MIL-91(Al) is heated in a vacuum at 393 K this water is removed to leave the dehydrated phase with a minor change in cell dimensions but with slightly broadened XRD peaks (Figure 5). This can be rehydrated upon standing in moist air to give the original phase.  $N_2$  adsorption on the dehydrated solid gives a type I isotherm that indicates the material has a Langmuir surface area close to  $500 \text{ m}^2 \cdot \text{g}^{-1}$  and a micropore volume of  $0.195 \text{ cm}^3 \cdot \text{g}^{-1}$  (Figure 6). TGA shows a distinct weight loss event between 490 and 550 K, which by analogy with other porous aluminum phosphonates with the same Al–OH–Al chains is likely to be from dehydroxylation and subsequent water loss (observed wt loss %, 5.2; calculated, 5.7%). At higher temperatures the organic ligand breaks down, and the solid becomes X-ray amorphous.

**MIL-91(Ti).** The structure of MIL-91(Ti) is confirmed by successful Rietveld refinement of the X-ray powder profile, in which the AlOH units are replaced by TiO units to maintain charge balance. Bond lengths determined for MIL-91(Ti) are acceptable, given the limitations of powder

**Table 2.** Atomic Coordinates ( $\times 10^4$ ;  $\text{\AA}^2$ ) for (a) MIL-91(Ti) and (b) MIL-91(Al)

atom	<i>x</i>	<i>y</i>	<i>z</i>	occupancy <sup>a</sup>
(a) MIL-91(Ti)				
Ti	3/4	3/4	1/2	
P(1)	0.343(1)	0	0.701(1)	
P(2)	0.320(1)	0	0.297(1)	
O(1)	0.223(1)	0	0.532(1)	
O(2)	0.331(1)	0.182(2)	0.629(2)	
O(3)	0.304(1)	0.158(2)	0.367(2)	
O(4)	0.419(1)	0	0.740(2)	
O(5)	0.287(1)	0	0.175(2)	
N(1)	0.469(1)	0	0.381(2)	
C(1)	0.504(1)	0.178(2)	0.433(1)	
C(2)	0.411(1)	0	0.273(2)	
N(2)	0.261(1)	0.195(3)	0.878(1)	50%
C(3)	0.294(1)	0	0.827(1)	
C(4)	0.320(1)	0.270(4)	0.959(2)	50%
C(5)	0.202(1)	0.111(3)	0.949(2)	50%
Ow(1)	0.400(1)	1/2	0.307(3)	
Ow(2)	0.002(1)	0	0.840(2)	
Ow(3)	0	-0.307(2)	0	
Ow(4)	0.371(2)	1/2	0.704(4)	62.6%
(b) MIL-91(Al)				
Al	3/4	3/4	1/2	
P(1)	0.332(1)	0	0.705(1)	
P(2)	0.340(1)	0	0.305(1)	
O(1)	0.215(1)	0	0.541(1)	
O(2)	0.322(1)	0.175(3)	0.620(3)	
O(3)	0.314(1)	0.162(3)	0.365(2)	
O(4)	0.411(1)	0	0.730(3)	
O(5)	0.300(1)	0	0.193(1)	
N(1)	0.474(1)	0	0.378(2)	
C(1)	0.469(1)	0.176(3)	0.455(2)	
C(2)	0.431(1)	0	0.262(2)	
N(2)	0.248(1)	0.154(1)	0.885(1)	50%
C(3)	0.251(1)	0	0.794(1)	
C(4)	0.317(1)	0.201(5)	0.946(3)	50%
C(5)	0.186(2)	0.142(5)	0.966(2)	50%
Ow(1)	0.421(1)	1/2	0.695(3)	
Ow(2)	0.025(2)	0	0.824(3)	
Ow(3)	0	-0.313(3)	0	

<sup>a</sup> Values based on structure refinement for the free water molecules.

**Table 3.** Principal Bond Lengths for (a) MIL-91(Ti) and (b) MIL-91(Al)

(a) MIL-91(Ti)			
Ti–O(1) ( $\times 2$ )	1.88(1)	Ti–O(2) ( $\times 2$ )	2.16(2)
Ti–O(3) ( $\times 2$ )	2.01(2)		
P(1)–O(2) ( $\times 2$ )	1.54(2)	P(1)–O(4)	1.52(2)
P(1)–C(3)	1.78(2)		
P(2)–O(3) ( $\times 2$ )	1.42(2)	P(2)–O(5)	1.51(2)
P(2)–C(2)	1.81(2)		
N(1)–C(1)	1.53(2)	N(1)–C(2)	1.64(3)
C(1)–C(1)	1.56(2)		
N(2)–C(3)	1.63(2)	N(2)–C(4)	1.54(3)
N(2)–C(5)	1.56(3)	C(4)–C(5)	1.43(3)
(b) MIL-91(Al)			
Al–O(1) ( $\times 2$ )	1.91(1)	Al–O(2) ( $\times 2$ )	1.98(2)
Al–O(3) ( $\times 2$ )	2.05(2)		
P(1)–O(2) ( $\times 2$ )	1.55(2)	P(1)–O(4)	1.52(2)
P(1)–C(3)	1.85(2)		
P(2)–O(3) ( $\times 2$ )	1.40(2)	P(2)–O(5)	1.47(2)
P(2)–C(2)	1.80(2)		
N(1)–C(1)	1.50(2)	N(1)–C(2)	1.54(3)
C(1)–C(1)	1.53(3)		
N(2)–C(3)	1.48(2)	N(2)–C(4)	1.50(3)
N(2)–C(5)	1.50(3)	C(4)–C(5)	1.48(3)

data analysis (Ti–O, 1.88–2.16  $\text{\AA}$ ; P–O, 1.42–1.54  $\text{\AA}$ ; P–C, 1.78–1.82  $\text{\AA}$ ).

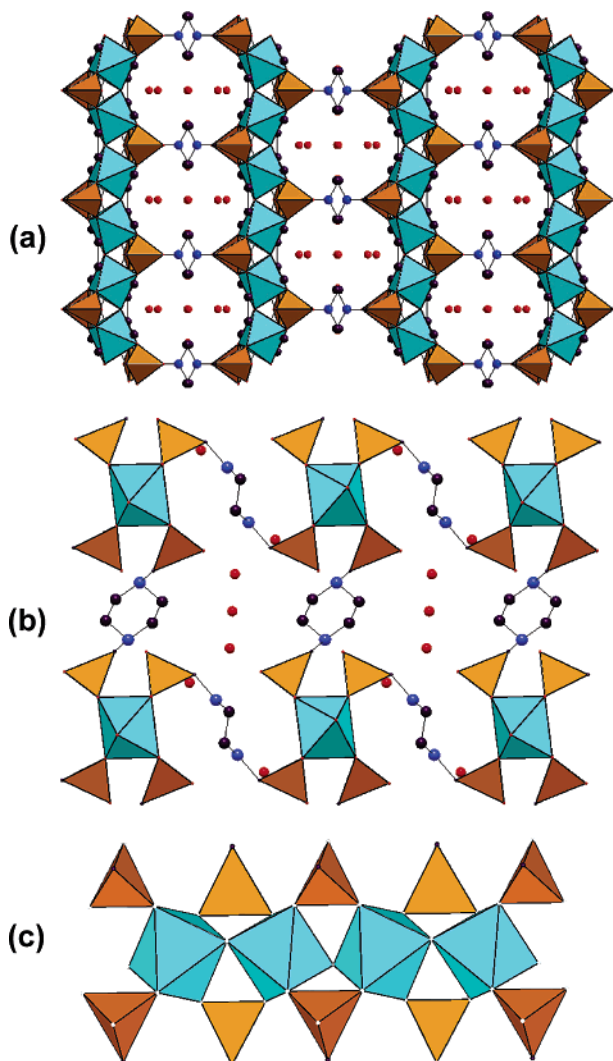


**Figure 2.** Structure of MIL-91 viewed (a) along the *c* axis and (b) along the *b* axis. For clarity, only one set of the two symmetry-equivalent (but half-occupied) sets of diphosphonate ligands connecting octahedral chains along *c* are shown. (c) A corner-sharing chain of MO<sub>6</sub> octahedra. Titanium octahedra, phosphorus tetrahedra, oxygen, nitrogen, and carbon atoms are in cyan, orange, red, blue, and purple, respectively.

The inorganic chains are similar to the tancoite-type chains encountered previously within the monodimensional titanium diphosphonates MIL-10<sup>20</sup> and in some templated metallo-phosphates.<sup>32,33</sup> In MIL-10, the two PO<sub>3</sub>C groups from the same diphosphonate unit are bound to the same titanyl chain giving a one-dimensional structural unit whereas in MIL-91(Ti) these groups connect neighboring inorganic chains along the *a* and *c* axes to produce a hybrid three-dimensional structure; this difference in connection mode for the diphosphonate unit derives from the segregation of the inorganic subnetwork and the organic moieties. In the layered titanium phosphates MIL-28<sup>32,33</sup> tancoite chains were related in one direction only by isolated titanium octahedra to form an inorganic layer with free water molecules and organic molecules filling pores defined by the interlayer space and the perforated layers. In MIL-91, the isolated titanium octahedra present in MIL-28 are replaced by diphosphonate groups.

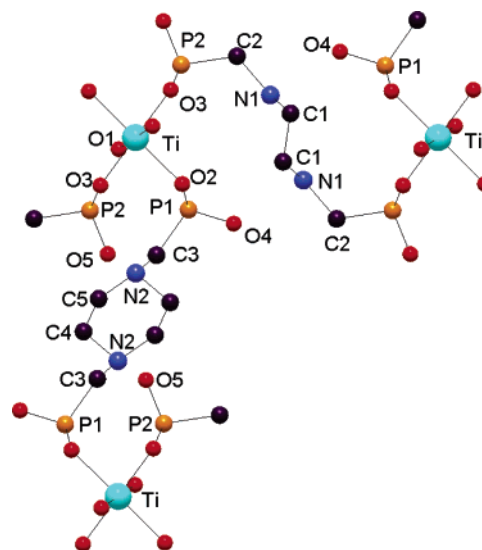


**Figure 3.** View of the structural subunit of MIL-91. Titanium octahedra, phosphorus tetrahedra, oxygen, nitrogen, and carbon atoms are in cyan, orange, red, blue, and purple, respectively.

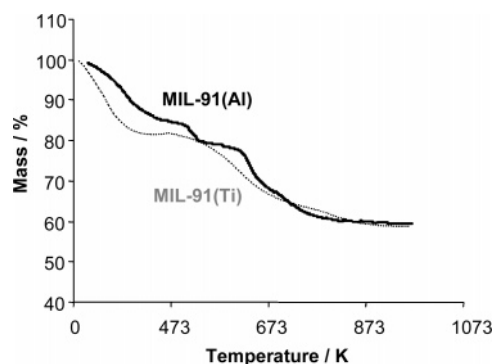


**Figure 4.** TGA of MIL-91 materials under flowing oxygen: (a) MIL-91-(Al), black full line; (b) MIL-91(Ti), gray dots.

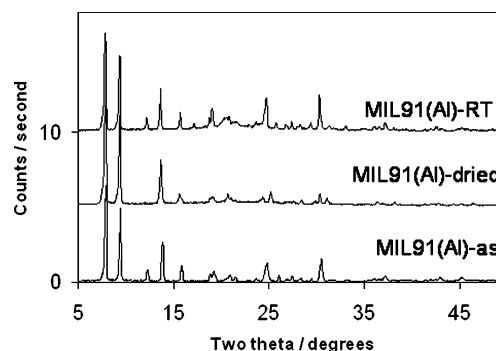


**Figure 5.** XRD of MIL-91(Al): as-prepared (bottom), before and after dehydration at 423 K (middle) and after re-hydration at room temperature (top).

TGA and X-ray thermodiffraction of MIL-91(Ti) (Figure 7) indicates that the structure loses the physisorbed water but remains crystalline up to 480 K. The water loss of ~18% occurring before 373 K is accompanied by a unit cell contraction of ~3% and a strong increase in the intensity of the X-ray peaks. Upon cooling to room temperature in moist air, MIL-91(Ti) rehydrates reversibly with no loss of crystallinity. At higher temperatures, the structure collapses and the dense TiP<sub>2</sub>O<sub>7</sub> solid crystallizes (observed weight loss, 29%; calculated, 28%). As for the aluminum form, the structure's rigidity upon water loss (compared to other hybrid

(32) Riou-Cavellec, M.; Serre, C.; Grenèche, J. M.; Férey, G. *C. R. Acad. Sci., Ser. IIC* **1999**, *2*, 85.

(33) Serre, C.; Taulelle, F.; Férey, G. *Chem. Mater.* **2002**, *14*, 998.

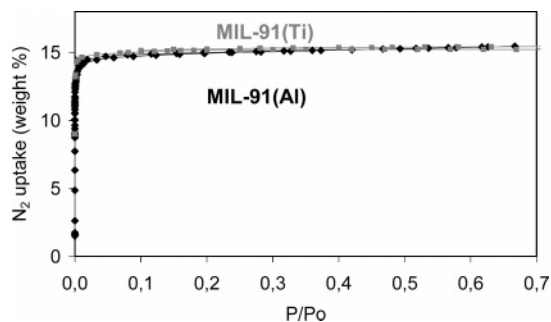


**Figure 6.** N<sub>2</sub> adsorption isotherms of MIL-91(Ti) (grey) and MIL-91(Al) (black) at 77 K ( $P_0 = 1$  atm.).

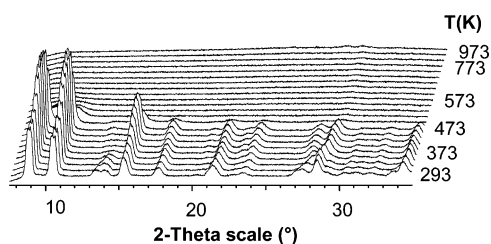


**Figure 7.** X-ray thermodiffraction of MIL-91(Ti) under an air atmosphere.

solids which show very large changes in volume)<sup>34</sup> can be attributed to the presence of strong H bonds between the terminal P=O groups and the protonated amino groups of the piperazine spacer. Thus, a noticeable porosity was expected for MIL-91 because a pore size of  $\sim 3.5 \times 4.0 \text{ \AA}^2$  was estimated, based on the structure of the as-synthesized solid. Nitrogen adsorption (and desorption) were, therefore, performed on a sample of MIL-91(Ti) outgassed at 473 K under vacuum, which indicated that this solid is microporous with a type I isotherm, a Langmuir surface area of  $500 \text{ m}^2 \cdot \text{g}^{-1}$ , and a pore volume close to  $0.19 \text{ cm}^3 \cdot \text{g}^{-1}$  (Figure 6).

The  $^{13}\text{C}\{^1\text{H}\}$  CPMAS NMR experiment of MIL-91(Ti) leads to a very broad peak at 51.8 ppm due to the different methylenic carbons ( $\text{CH}_2$ ) present in the organic part of the phosphonate groups (Figure 8a). The severe broadening of this signal, preventing distinction between different kinds of carbon sites, may result from static disorder in the organic chains within the structure. The  $^1\text{H}$  NMR spectrum of MIL-91(Ti) after dehydration at 373 K overnight and subsequent treatment at 423 K for 2 h prior to NMR measurement is displayed in Figure 8b. The sample was packed into the NMR rotor as fast as possible to avoid rehydration. This procedure allowed removing the dominant signal of water at 4.8 ppm, which overlaps with the other signals. At least two resolved peaks at  $\delta = 13.2$  and 3.4 can be distinguished. The latter is a composite signal that can account for the different types of methylene protons present. According to the low field chemical shift, the former can be assigned to acidic protons in the form of terminal P–OH rather than protonated amine groups, which usually resonate around 7 ppm. This suggests that protons in MIL-91(Ti) can reside on either terminal phosphonate P=O groups or on the amine. The  $^{31}\text{P}$  MAS NMR spectrum of MIL-91(Ti) shows two

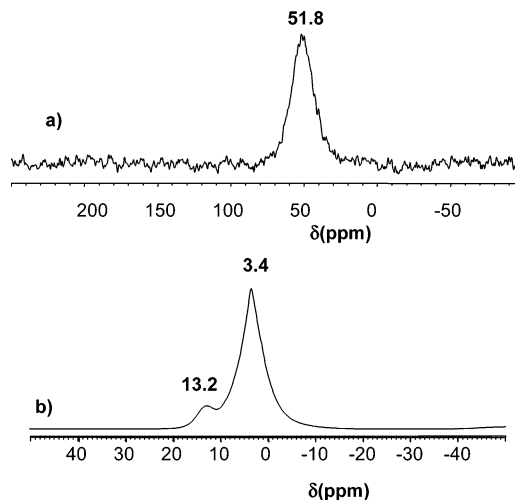


**Figure 8.**  $^{13}\text{C}\{^1\text{H}\}$  CPMAS (a) and  $^1\text{H}$  MAS (b) NMR spectra of MIL-91(Ti) acquired at spinning speeds of 5 and 30 kHz, respectively.

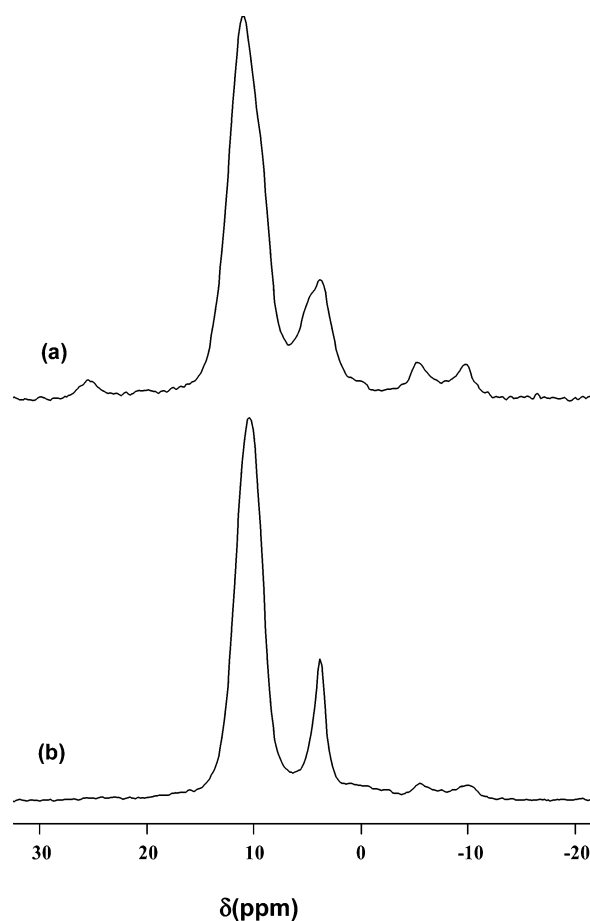


**Figure 9.**  $^{31}\text{P}$  MAS NMR spectra of MIL-91(Ti) after (a) and before (b) dehydration at 373 K overnight and subsequent treatment at 423 K for 2 h. The spinning speed was 30 kHz.

distinct peaks at around 4 and 11 ppm (Figure 9). Usually, chemical shift values of phosphonates fall in the broad range from 2 to 27 ppm (reference 85%  $\text{H}_3\text{PO}_4$ ).<sup>35–38</sup> Two other small peaks were observed at around  $-5$  and  $-10$  ppm assigned to phosphate impurities. To check that the two

(34) Serre, C.; Millange, F.; Thouvenot, C.; Nogues, M.; Marsolier, G.; Louër, D.; Férey, G. *J. Am. Chem. Soc.* **2002**, *124*, 13519.

(35) Lima, C. B. A.; Airoldi, C. *Solid State Sci.* **2002**, *4*, 1321–1329.

(36) Lima, C. B. A.; Airoldi, C. *Int. J. Inorg. Mater.* **2001**, *3*, 907–914.

(37) Sasaki, D. Y.; Alam, T. M. *Chem. Mater.* **2000**, *12*, 1400–1407.

(38) Leenstra, W. R.; Amicangelo, J. C. *Inorg. Chem.* **1998**, *37*, 5317–5323.

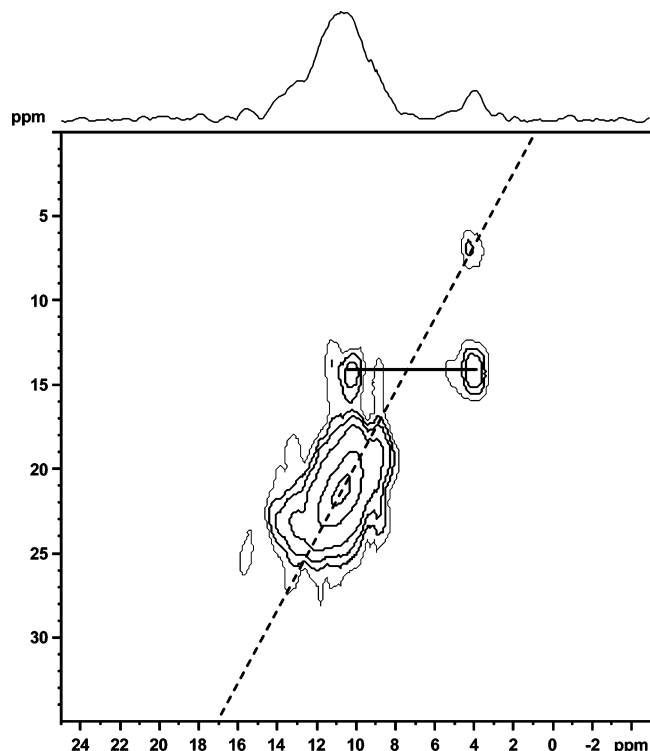


**Figure 10.**  $^{31}\text{P}$  DQ MAS NMR correlation spectra of MIL-91(Ti) obtained using the POSTC7 sequence. The spinning speed was 12.5 kHz.

largest signals belong to the same phase, a two-dimensional  $^{31}\text{P}$ – $^{31}\text{P}$  DQ NMR experiment was undertaken. The spectrum, depicted in Figure 10, showed clearly that the signals are correlated, indicating the existence of dipolar through-space interactions. This result confirms that these signals correspond to two neighboring phosphorus sites present in MIL-91, ruling out the possible assignment of the smaller signal to an impurity and suggesting they might relate to protonated and nonprotonated phosphonate groups in the structure. The two main signals remain upon dehydration, with some associated broadening. Using cadmium and ethylenediamine (*N,N'*-bismethylenediphosphonic acid), Clearfield and co-workers obtained a hybrid solid and extensively studied the state of protonation of the bisphosphonate groups on this solid. They showed using a combined IR–NMR study that the latter exhibit a zwitterionic structure ( $\text{NH}_2^+ - \text{CH}_2\text{P}(\text{O}_2\text{Cd}_2)\text{O}_2^-$ ) similar to that of the initial aminophosphonic acid.<sup>39</sup>

#### 4. Summary

The aluminum and titanium diphosphonates of the type MIL-91 have closely similar structures which are made up of chains of corner-sharing metal octahedral along the *b* axis linked by *N,N'*-piperazinebismethylenephosphonate ligands along the *a* and *c* axes. In the hydrated form the framework structures take up water in the channels that run parallel to the inorganic chains. Both structures lose the physisorbed water upon heating at about 400 K with retention of the framework structure. The resulting one-dimensional small pore channel system is able to adsorb nitrogen at 77 K with Langmuir surface areas close to  $500 \text{ m}^2 \cdot \text{g}^{-1}$  and pore volumes close to  $0.19 \text{ cm}^3 \cdot \text{g}^{-1}$ . Heating above 473 K results in loss of crystallinity for both materials.

MIL-91 is a significant new aluminum phosphonate, because it is only the third such material (after the microporous AlMePO- $\alpha$  and - $\beta$  polymorphs of  $\text{Al}_2(\text{CH}_3\text{PO}_3)_3$ ) for which porosity to molecules other than water has been demonstrated.<sup>40,41</sup> Also, although several porous tetravalent metallodiphosphonates have been reported, mostly using zirconium, MIL-91(Ti) is the first titanium diphosphonate for which well-defined porosity has been observed. Indeed, titanium-based hybrid solids are still rare, and the porosity reported here is much higher than those observed for the well-known layered  $\alpha$ -<sup>42</sup> or  $\gamma$ -<sup>43</sup> TiP or ZrP solids and close to the best results obtained previously with a zirconium biphenyldiphosphonate (surface area between 300 and  $430 \text{ m}^2 \cdot \text{g}^{-1}$ ).<sup>19</sup>

**Acknowledgment.** We gratefully acknowledge the help of Dr. P. Wormald (St. Andrews) and Dr. Claudia Morais (Versailles) in collecting some of the NMR data presented.

**Supporting Information Available:** Crystallographic information (CIF). This material is available free of charge via the Internet at <http://pubs.acs.org>.

CM052149L

- (39) Bakhmutova-Albert, E. V.; Betsaoui, N.; Bakhmutova, V. I.; Clearfield, A.; Rodriguez, A. V.; Llanova, R. *Inorg. Chem.* **2004**, *43*, 1264.  
 (40) Maeda, K.; Akimoto, J.; Kiyozumi, Y.; Mizukami, F. *J. Chem. Soc., Chem. Commun.* **1995**, *10*, 1033.  
 (41) Maeda, K.; Akimoto, J.; Kiyozumi, Y.; Mizukami, F. *Angew. Chem., Int. Ed. Engl.* **1995**, *34*, 1199.  
 (42) Clearfield, A.; Stynes, J. A. *J. Inorg. Nucl. Chem.* **1964**, *26*, 117.  
 (43) Alluli, S.; Ferragina, C.; La Ginestra, C.; Massucci, M. A.; Tomassini, N. *J. Inorg. Nucl. Chem.* **1977**, *39*, 1043.